the packing of equivalent paired stacks of the (*C''*) type. The inference is that (*C'*) is of lower energy than (*C''*) and that it is energetically favourable to convert half of the molecules into (*C''*) to relieve packing strain, but unfavourable to convert them all into (*C''*). The result is a molecular complex in which the total molecular and packing strain energy is a minimum.

References

ALTONA, C. & SUNDARALINGAM, M. (1972). *J. Amer. Chem. Soc.* **94**, 8205–8212.

BISCHOFBERGER, K., BRINK, A. J., DE VILLIERS, O. G., HALL, R. H. & JORDAAN, A. (1977). *J. Chem. Soc. Perkin* I. To be published.

BOEYENS, J. C. A. (1977). *Acta Cryst.* A**33**. To be published.

CAHN, R. S., INGOLD, C. K. & PRELOG, V. (1956). *Experientia*, **12**, 81–94.

CREMER, D. & POPLE, J. A. (1975). *J. Amer. Chem. Soc.* **97**, 1354–1358.

HOPPE, D. (1974). *Angew. Chem. Int. Ed.* **13**, 789–804.

SHELDRICK, G. M. (1976). Private communication.

SUHADOLNIK, R. J. (1970). *Nucleoside Antibiotics*, p. 218. New York: John Wiley.

Acta Cryst. (1977). B**33**, 3066–3072

Positional Disorder and Non-Stoichiometry in $Cu_{2-x}Mo_3S_4$ Compounds. I. Single-Crystal Studies of $Cu_{2-x}Mo_3S_4$ ($x = 1{\cdot}1, 0{\cdot}62, 0{\cdot}53, 0{\cdot}17$) at Room Temperature

BY KLAUS YVON

Laboratoire de Cristallographie aux Rayons X, 24 quai Ernest Ansermet, Université de Genève, CH-1211 Genève 4, Switzerland

AND ALAIN PAOLI, RENÉ FLÜKIGER AND ROGER CHEVREL*

Département de Physique de la Matière Condensée, 24 quai Ernest Ansermet, Université de Genève, CH-1211 Genève 4, Switzerland

(*Received* 24 *February* 1977; *accepted* 1 *April* 1977)

The results of an X-ray investigation of $Cu_{2-x}Mo_3S_4$ alloys as a function of the Cu concentration are reported. The structure is described in terms of a model consisting of rigid Mo_6S_8 building blocks with a rhombohedral stacking. The building blocks are cubes of S atoms which are centred by an octahedron formed by Mo atoms. At room temperature, the Cu atoms are found in tetrahedral interstices of the S atom network. 12 of these holes are very close together and form a cluster. These cluster sites correspond to two sixfold equivalent crystallographic positions which are filled to a different extent if the Cu content of the compound is increased. The maximum possible Cu occupation is four atoms per cluster which corresponds to the formula $Cu_2Mo_3S_4$. The Mo:S ratio was found to be constant in all compounds. Analyses of the thermal parameters suggest that the Mo_6 octahedra form stable units which vibrate preferentially around and along the ternary axis and that the Cu atoms of the first site undergo large anisotropic oscillations (r.m.s. amplitude = 0·3 Å) in the direction of the Cu atoms of the second site and *vice versa*. Cu atoms on peripheral sites that belong to adjacent clusters are separated by only 2·1–2·4 Å. Ionic d.c. conduction is therefore possible. Variations in the interatomic distances with increasing Cu content correspond to a general expansion of the structure except for the Mo–Mo contacts which decrease. This contraction is interpreted by assuming partially filled *d* orbitals localized on the Mo atoms which become more populated with increasing Cu concentration, the latter element acting as an electron donor. The ionic formula $Cu_4^+[Mo_6^{2+}S_8^{2-}]^{4-}$ is proposed.

Introduction

Ternary Mo sulphides of formula $M_xMo_3S_4$, M = transition element, metal or rare-earth element, $0 < x \leq 2$ (Chevrel, Sergent & Prigent, 1971; Fischer, Treyvaud, Chevrel & Sergent, 1975), are of interest because of their outstanding physical properties at low temperatures. The compounds are generally good superconductors (Matthias, Marezio, Corenzwit, Cooper & Barz, 1972), yield exceptionally high critical fields (Fischer, 1974) and have a marked pressure

* Present address: Université de Rennes, Laboratoire de Chimie Minérale B, Laboratoire Associé au CNRS n° 254, Rennes CEDEX 35031, France.

dependence of the superconducting transition temperature (Shelton, Lawson & Johnston, 1975). Furthermore, the possibility of substituting S by other chalcogenides and *M* by a great variety of elements that differ in atomic number, size, electronegativity and concentration is an attractive feature in the study of their physical properties. Such substitution was found to have important effects on the electrical resistivity (Lawson, 1972), on the heat capacity (Viswanathan & Lawson, 1972), on the critical temperature and on the critical field (Fischer, Odermatt, Bongi, Jones, Chevrel & Sergent, 1973). Lattice instabilities were also found to exist at low temperatures but only in compounds containing small cations such as Co (Lawson, 1972) and Cu (Flükiger, Devantay, Jorda & Muller, 1977). In compounds containing large cations such as Pb and Sn, softening of the lattice was observed by Mössbauer and inelastic neutron scattering studies (Kimball, Weber, Van Landuyt, Fradin, Dunlap & Shenoy, 1976; Bader, Knapp, Sinha, Schweiss & Renker, 1976). These observations led to the assumption of a molecular crystal model to interpret the lattice dynamics. It consists of rigid Mo_6S_8 building blocks which are responsible for torsional modes and of interstitial Pb and Sn atoms which are responsible for translational modes. The latter atoms are believed to be only weakly bound and to undergo large anharmonic displacements of increasing amplitude at lower temperatures. No agreement exists however on which mode is critical for the magnitude of the superconducting transition temperature.

Single-crystal X-ray studies have been carried out for a few compounds such as $Pb_{0.46}Mo_3S_{3.75}$ (Marezio, Dernier, Remeika, Corenzwit & Matthias, 1973), $Pb_{0.46}Mo_3S_4$ (Guillevic, Lestrat & Grandjean, 1976), $NiMo_3S_4$, $Ni_{0.70}Mo_3S_4$, $Co_{0.80}Mo_3S_4$ and $Fe_{0.66}Mo_3S_4$ (Guillevic, Bars & Grandjean, 1973, 1976). These compounds were found to be isostructural as far as the overall arrangement of the Mo_6S_8 building blocks is concerned, but exhibit differences in the distribution of the third alloying component. This distribution seems to depend mainly on the size of the cations, since Pb was found to be eightfold coordinated whereas Ni, Co and Fe prefer tetrahedral S environments. The type of insertion also affects slightly the packing of the Mo_6S_8 units, since rhombohedral angles smaller than 90° are observed for compounds containing large cations and angles greater than 90° if the interstitial atom is small. Although these structural changes are relatively minor, they result in important variations of the physical properties. Accurate single-crystal X-ray studies are therefore desirable to correlate structural parameters, such as interatomic distances or vibrational amplitudes, with physical properties. The object of the present work is to study the influence of the gradual insertion of Cu on the structure of the host lattice and the distribution and thermal parameters of the dissolved atoms.

Experimental

All compounds were prepared by synthesis from the elements. $Cu_{0.90}Mo_3S_4$ was obtained by vapour transport and the other alloys by fusion of the prereacted components in a high-pressure argon furnace. Single crystals of regular shape were isolated for each compound and tested for their quality with azimuthal scans on a four-circle diffractometer. The crystals yielding the best results were retained and measured under identical experimental conditions with continuous θ–2θ scans. For each crystal 980 intensities were collected for one hemisphere in the sin θ/λ range 0·07 to 0·91 Å^{-1}. After averaging equivalent intensities 613 unique reflexions were obtained of which 507 had $I > 3\sigma(I)$. No correction was made for absorption. Refinement of the structure started from the positional parameters of Mo and S in $Ni_{0.70}Mo_3S_4$ (Guillevic, Bars & Grandjean, 1976). The Cu atoms were located on difference maps and the positional, occupational and anisotropic thermal parameters obtained by full-matrix least-squares refinement (XRAY system, 1976) with all data. The function minimized was $\Sigma w\Delta F^2$ where $w = 1/\sigma^2(F_o)$. Scattering factors and anomalous dispersion corrections were taken from *International Tables for*

Table 1. *Crystal data for* $Cu_{2-x}Mo_3S_4$ *compounds compared with* Mo_3S_4

	Mo_3S_4	$Cu_{0.90}Mo_3S_4$	$Cu_{1.38}Mo_3S_4$	$Cu_{1.47}Mo_3S_4$	$Cu_{1.83}Mo_3S_4$
Space group	$R\bar{3}$	$R\bar{3}$	$R\bar{3}$	$R\bar{3}$	$R\bar{3}$
a_{rh} (Å)	6·432	6·503 (1)	6·560 (1)	6·573 (1)	6·597 (1)
α (°)	91·34	94·93 (2)	95·51 (2)	95·56 (2)	95·58 (2)
a_{hex} (Å)	9·202	9·584 (2)	9·713 (2)	9·735 (2)	9·773 (2)
c_{hex} (Å)	10·877	10·250 (2)	10·213 (2)	10·221 (2)	10·255 (2)
V_{hex} (Å^3)	797·6	815·4	834·4	838·9	848·2
FW	416·1	473·3	503·7	509·4	531·0
D_x (g cm^{-3})	5·20	5·747	5·977	6·012	6·237
Z	6	6	6	6	6
μ (cm^{-1})	81·7	114·4	129·8	132·4	143·5
μR	0·3	0·27	0·15	0·23	0·15
Atomic volume (Å^3)	18·99	17·20	16·60	16·51	16·05

X-ray Crystallography (1974). The final $R = \Sigma|\Delta F|/\Sigma|F_o|$ for all four data sets was 0·03, including all reflexions.*

Results and discussion

The crystal data for the four compounds are summarized in Table 1 and the final atomic coordinates, occupancies and thermal parameters in Table 2. In both tables the corresponding parameters of Mo_3S_4 (Chevrel, Sergent & Prigent, 1971) have been included.

The stereoscopic view (Fig. 1) (Johnson, 1965) displays the essential features of the structure. A detailed view of the Cu atom arrangement is given in Fig. 2, showing the range of interatomic distances and the directions and amplitudes of the thermal vibrations. These drawings represent in a qualitative manner the structures of all four compounds. For a quantitative comparison Table 3 gives the bond lengths.

* A list of structure factors has been deposited with the British Library Lending Division as Supplementary Publication No. SUP 32630 (12 pp.). Copies may be obtained through The Executive Secretary, International Union of Crystallography, 13 White Friars, Chester CH1 1NZ, England.

Description of the structure

The atom arrangement is analogous to that reported for $NiMo_3S_4$ and $Ni_{0.7}Mo_3S_4$ (Guillevic, Bars & Grandjean, 1973, 1976). The S atoms form a three-dimensional anion network which is not close-packed since it results from stacking almost regular S_8 cubes along rhombohedral axes. The packing is such that the corners of one cube lie above the face centres of others. Each cube contains a Mo_6 octahedron oriented in such a way that all Mo atoms lie slightly outside and close to the middle of the faces. The resulting Mo_6S_8 building block has therefore almost cubic symmetry but the three-dimensional arrangement of these cubes evokes trigonal symmetry. The S atom network presents several tetrahedral interstices and one large hole formed by a cube of S atoms. This cube is centred on the origin of the unit cell and is compressed along the ternary axis in such a way that six equivalent tetrahedral interstices (type 1) result. Interstices of type 1 that belong to different cubes are interconnected by two equivalent interstices (type 2) which also have tetrahedral coordination.

Both type 1 and 2 interstices were found to be occupied by Cu. However, full occupancy of these sites

Table 2. *Positional* ($\times 10^5$), *occupational and thermal* ($Å^2 \times 10^4$) *parameters for* $Cu_{0.90}Mo_3S_4$, $Cu_{1.38}Mo_3S_4$, $Cu_{1.47}Mo_3S_4$ *and* $Cu_{1.83}Mo_3S_4$, *with their standard errors*

Anisotropic temperature factor is expressed as $\exp[-2\pi^2(U_{11}h^2a^{*2} + U_{22}k^2b^{*2} + U_{33}l^2c^{*2} + 2U_{12}hka^*b^* + 2U_{13}hla^*c^* + 2U_{23}klc^*b^*)]$. Space group $R\bar{3}$, hexagonal setting.

	$x(\sigma)$	$y(\sigma)$	$z(\sigma)$	Occupancy (σ)	$U_{11}(\sigma)$	$U_{22}(\sigma)$	$U_{33}(\sigma)$	$U_{12}(\sigma)$	$U_{13}(\sigma)$	$U_{23}(\sigma)$
$Cu_{0.90}Mo_3S_4$										
Mo	1590 (4)	16897 (5)	38904 (7)	1·00 (—)	70 (2)	77 (2)	55 (9)	35 (1)	−4 (1)	−8 (1)
S(1)	30973 (14)	27689 (14)	41183 (21)	1·00 (—)	87 (4)	100 (4)	65 (16)	47 (3)	10 (5)	16 (5)
S(2)	0 (—)	0 (—)	20152 (39)	1·00 (—)	129 (—)	129 (—)	25 (28)	65 (3)	0 (—)	0 (—)
Cu(1)	72662 (57)	48391 (53)	32913 (65)	0·26 (1)	333 (18)	294 (17)	229 (43)	204 (15)	−144 (20)	−120 (20)
Cu(2)	13211 (350)	22373 (372)	91000 (426)	0·04 (1)	518 (133)	544 (142)	801 (320)	359 (123)	−533 (174)	−406 (180)
$Cu_{1.38}Mo_3S_4$										
Mo	1484 (6)	16564 (6)	39103 (9)	1·00 (—)	63 (3)	73 (3)	53 (11)	35 (2)	−2 (2)	−2 (2)
S(1)	30754 (19)	27713 (20)	40970 (28)	1·00 (—)	88 (6)	99 (6)	96 (22)	50 (5)	2 (6)	14 (6)
S(2)	0 (—)	0 (—)	20195 (54)	1·00 (—)	133 (—)	133 (—)	19 (36)	67 (4)	0 (—)	0 (—)
Cu(1)	72529 (87)	48711 (83)	33172 (96)	0·24 (1)	412 (31)	436 (34)	420 (67)	261 (28)	−218 (34)	−95 (36)
Cu(2)	14694 (102)	23611 (90)	89666 (115)	0·22 (1)	444 (41)	280 (30)	393 (82)	227 (31)	−256 (44)	−203 (37)
$Cu_{1.47}Mo_3S_4$										
Mo	1456 (5)	16483 (5)	39165 (8)	1·00 (—)	67 (2)	68 (2)	45 (11)	33 (1)	−1 (2)	1.(2)
S(1)	30738 (15)	27676 (16)	40947 (24)	1·00 (—)	82 (5)	97 (5)	96 (19)	44 (4)	−5 (6)	17 (6)
S(2)	0 (—)	0 (—)	20218 (47)	1·00 (—)	137 (—)	137 (—)	92 (32)	68 (3)	0 (—)	0 (—)
Cu(1)	72397 (71)	48721 (72)	33428 (88)	0·22 (1)	311 (23)	400 (28)	370 (60)	202 (22)	−214 (28)	−114 (30)
Cu(2)	14859 (68)	23694 (68)	89510 (82)	0·27 (1)	469 (28)	423 (26)	549 (61)	275 (23)	−319 (33)	−277 (30)
$Cu_{1.83}Mo_3S_4$										
Mo	1418 (9)	16369 (9)	39282 (12)	1·00 (—)	59 (4)	59 (4)	69 (15)	30 (3)	−6 (3)	0 (3)
S(1)	30683 (30)	27780 (28)	40872 (35)	1·00 (—)	82 (10)	98 (10)	91 (26)	43 (9)	−3 (12)	46 (12)
S(2)	0 (—)	0 (—)	20153 (67)	1·00 (—)	160 (—)	160 (—)	20 (45)	80 (6)	0 (—)	0 (—)
Cu(1)	72377 (164)	48270 (139)	33242 (145)	0·23 (1)	476 (63)	635 (76)	591 (100)	313 (70)	−130 (61)	−84 (67)
Cu(2)	15164 (58)	24085 (65)	89202 (68)	0·38 (1)	283 (24)	365 (29)	316 (29)	140 (21)	−165 (28)	−181 (28)

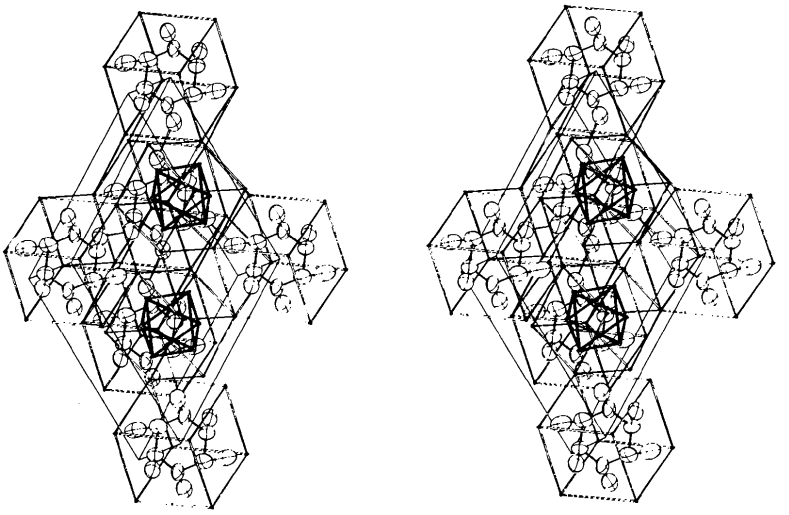

Fig. 1. Stereoscopic pair of $Cu_{2-x}Mo_3S_4$. The dark lines correspond to Mo–Mo contacts and outline Mo_6 octahedra. The lighter double lines contouring cubes correspond to S–S contacts. The Cu atoms are represented by large ellipsoids which are interconnected to form clusters of 12 atoms. Each cluster is connected *via* Cu–Cu contacts to six other clusters which form a three-dimensional network. The thermal ellipsoids have been drawn to scale for the Cu atoms only (70% probability). The other atoms are represented by arbitrary values of thermal parameters.

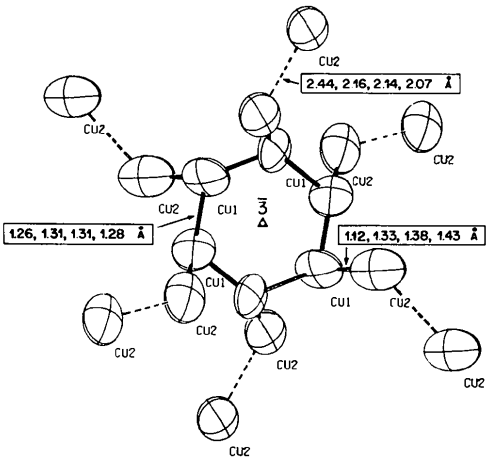

Fig. 2. Perspective view of the cluster of 12 partially occupied Cu positions. The six innermost positions correspond to site 1 and the six positions further out to site 2. The nearest-atom positions of adjacent Cu clusters are also represented and correspond to the six peripheral atoms. The thermal ellipsoids are drawn on a 70% probability scale and the distances between nearest-atom sites are indicated for the four compositions in the order $Cu_{0.90}Mo_3S_4$, $Cu_{1.38}Mo_3S_4$, $Cu_{1.47}Mo_3S_4$ and $Cu_{1.83}Mo_3S_4$.

is not possible because of atom overlap: the distances between equivalent atoms on site 1 and between the origin and these sites are very small (1·12–1·43 and 1·27–1·31 Å depending on the Cu concentration). Assuming an ionic radius of 0·96 Å for Cu^+ one expects only three of the six equivalent sites to be occupied on average (Fig. 3). The distance between site 1 and site 2 is also very small (1·12–1·42 Å, depending on the Cu concentration) and both sites cannot be occupied simultaneously. Because of this overlap the two sixfold crystallographic sites may be considered to form clusters of 12 vacancies. The Cu atoms inside such a cluster may occupy either one of these vacancies (static disorder) or may occupy them simultaneously with two different degrees of probabilities (dynamic disorder). By comparison, the Cu sites belonging to different clusters are much further apart, the minimum distances being 2·07–2·44 Å [distances between Cu(2) sites], depending on the Cu concentration.

The maximum possible Cu concentration in one cluster is six Cu atoms. This leads to a hypothetical phase limit at the composition $Cu_3Mo_3S_4$. However, the real phase limit is known to be $Cu_2Mo_3S_4$ (Chevrel, 1974), which means that only four Cu atoms occupy one cluster of 12 available sites.

Occupancy of Cu *sites*

Fig. 3 represents the variation of the population parameters of the two Cu sites as a function of the overall Cu concentration. As one expects, the average occupancy increases with concentration but the detailed balance of occupancy between sites 1 and 2 is apparently more complex. In fact, the Cu atoms are not evenly distributed over the two sites. At low Cu concentrations, the site close to the origin is clearly preferred whereas the other site is rapidly filled at higher Cu concentrations. This increase can readily be interpreted as the result of electrostatic repulsion which forces the ions toward peripheral sites in the cluster.

The variation of occupancy of the inner site is more difficult to interpret since it results from two counteracting forces which cannot be evaluated numerically. The first is related to the overlap of atoms on site 1 and site 2 and acts in the direction of decreasing occupancy. The other originates from electrostatic repulsion be-

Table 3. *Interatomic distances* (Å) *and their estimated standard deviations for* $Cu_{0.90}Mo_3S_4$, $Cu_{1.38}Mo_3S_4$, $Cu_{1.47}Mo_3S_4$ *and* $Cu_{1.83}Mo_3S_4$ *up to* 3·775 Å

	$Cu_{0.90}Mo_3S_4$	$Cu_{1.38}Mo_3S_4$	$Cu_{1.47}Mo_3S_4$	$Cu_{1.83}Mo_3S_4$
Mo–Mo	2× 2·683 (2)	2× 2·671 (2)	2× 2·665 (2)	2× 2·659 (2)
	2× 2·752 (2)	2× 2·708 (2)	2× 2·697 (2)	2× 2·681 (2)
	3·237 (2)	3·330 (2)	3·353 (2)	3·389 (2)
–S(1)	2·407 (2)	2·420 (3)	2·422 (3)	2·433 (4)
	2·443 (2)	2·466 (2)	2·465 (2)	2·479 (3)
	2·478 (2)	2·493 (2)	2·498 (2)	2·502 (3)
	2·494 (2)	2·527 (3)	2·541 (2)	2·551 (4)
–S(2)	2·469 (4)	2·471 (5)	2·473 (4)	2·491 (6)
–Cu(2)	3·163 (11)	3·183 (17)	3·186 (14)	3·250 (30)
–Cu(2)	3·031 (66)	3·095 (18)	3·114 (13)	3·130 (11)
	3·196 (46)	3·083 (13)	3·076 (9)	3·074 (8)
	3·247 (71)	3·216 (19)	3·217 (14)	3·220 (13)
S(1)–Mo	2·407 (2)	2·420 (3)	2·422 (3)	2·433 (4)
	2·443 (2)	2·466 (2)	2·465 (2)	2·479 (3)
	2·478 (2)	2·493 (2)	2·498 (2)	2·502 (3)
	2·494 (2)	2·527 (3)	2·541 (2)	2·551 (4)
–S(1)	2× 3·353 (4)	2× 3·396 (5)	2× 3·402 (4)	2× 3·424 (6)
	2× 3·513 (4)	2× 3·502 (4)	2× 3·506 (4)	2× 3·514 (5)
	2× 3·569 (3)	2× 3·605 (3)	2× 3·610 (3)	2× 3·625 (6)
	3·775 (3)	3·755 (4)	3·763 (3)	3·748 (5)
–S(2)	3·426 (3)	3·494 (4)	3·503 (3)	3·525 (5)
	3·553 (3)	3·554 (5)	3·555 (4)	3·569 (5)
	3·669 (3)	3·708 (3)	3·719 (3)	3·723 (4)
–Cu(1)	2·321 (8)	2·347 (13)	2·349 (11)	2·390 (22)
	2·343 (9)	2·354 (15)	2·357 (12)	2·399 (26)
	3·473 (7)	3·573 (10)	3·598 (9)	3·590 (18)
	3·563 (6)	3·603 (8)	3·595 (7)	3·615 (14)
	3·637 (7)	3·613 (10)	3·596 (9)	3·649 (16)
–Cu(2)	2·269 (51)	2·381 (13)	2·401 (9)	2·419 (9)
	2·271 (50)	2·298 (13)	2·304 (10)	2·319 (9)
	2·729 (36)	2·575 (10)	2·562 (7)	2·529 (7)
	3·268 (42)	3·313 (12)	3·313 (8)	3·349 (8)
	3·640 (47)	3·513 (14)	3·503 (9)	3·484 (9)
S(2)–Mo	3× 2·469 (4)	3× 2·471 (5)	3× 2·473 (4)	3× 2·491 (6)
–S(1)	3× 3·426 (3)	3× 3·494 (4)	3× 3·503 (3)	3× 3·525 (5)
	3× 3·553 (3)	3× 3·554 (5)	3× 3·555 (4)	3× 3·569 (5)
	3× 3·669 (3)	3× 3·708 (3)	3× 3·719 (3)	3× 3·723 (4)
–Cu(1)	3× 2·382 (7)	3× 2·427 (10)	3× 2·456 (10)	3× 2·421 (16)
	3× 2·456 (7)	3× 2·455 (10)	3× 2·439 (9)	3× 2·437 (21)
–Cu(2)	3× 2·189 (34)	3× 2·244 (9)	3× 2·251 (7)	3× 2·274 (6)
	3× 3·524 (40)	3× 3·707 (12)	3× 3·732 (11)	3× 3·785 (10)
	3× 3·706 (32)	3× 3·644 (8)	3× 3·645 (7)	3× 3·625 (6)
Cu(1)–Mo	3·163 (11)	3·183 (17)	3·186 (14)	3·250 (30)
–S(1)	2·321 (8)	2·347 (13)	2·349 (11)	2·390 (22)
	2·343 (9)	2·354 (15)	2·357 (12)	2·399 (26)
	3·473 (7)	3·573 (10)	3·598 (9)	3·590 (18)
	3·563 (6)	3·603 (8)	3·595 (7)	3·615 (14)
	3·637 (7)	3·613 (10)	3·596 (9)	3·649 (16)
–S(2)	2·382 (7)	2·427 (10)	2·456 (10)	2·421 (16)
	2·456 (7)	2·455 (10)	2·439 (9)	2·437 (21)
–Cu(1)	2×1·261 (12)	2× 1·306 (18)	2× 1·311 (15)	2× 1·276 (32)
	2×2·180 (8)	2× 2·261 (12)	2× 2·271 (10)	2× 2·210 (22)
	2·518 (7)	2·611 (11)	2·623 (10)	2·552 (18)
–Cu(2)	1·122 (38)	1·330 (13)	1·377 (11)	1·426 (15)
	1·678 (63)	1·766 (19)	1·752 (15)	1·823 (27)
	2·145 (57)	2·366 (18)	2·390 (14)	2·424 (21)
	2·691 (39)	2·844 (11)	2·860 (9)	2·887 (19)
	3·005 (52)	3·251 (17)	3·290 (13)	3·299 (19)
	3·254 (32)	3·452 (11)	3·464 (9)	3·489 (13)
	3·449 (39)	3·297 (13)	3·304 (11)	3·285 (15)

Table 3 (*cont.*)

	$Cu_{0.90}Mo_3S_4$	$Cu_{1.38}Mo_3S_4$	$Cu_{1.47}Mo_3S_4$	$Cu_{1.83}Mo_3S_4$
Cu(2)–Mo	3·031 (66)	3·095 (18)	3·114 (13)	3·130 (11)
	3·196 (46)	3·083 (13)	3·076 (9)	3·074 (8)
	3·247 (71)	3·216 (19)	3·217 (14)	3·220 (13)
–S(1)	2·269 (51)	2·381 (13)	2·401 (9)	2·419 (9)
	2·271 (50)	2·298 (13)	2·304 (10)	2·319 (9)
	2·729 (36)	2·575 (10)	2·562 (7)	2·529 (7)
	3·268 (42)	3·313 (12)	3·313 (8)	3·349 (8)
	3·640 (47)	3·513 (14)	3·503 (9)	3·484 (9)
–S(2)	2·189 (34)	2·244 (9)	2·251 (7)	2·274 (6)
	3·524 (40)	3·707 (12)	3·732 (9)	3·784 (9)
	3·706 (32)	3·644 (8)	3·645 (7)	3·625 (6)
–Cu(1)	1·122 (38)	1·330 (13)	1·377 (11)	1·426 (15)
	1·678 (63)	1·766 (19)	1·752 (15)	1·823 (27)
	2·145 (57)	2·366 (18)	2·390 (14)	2·424 (21)
	2·691 (39)	2·844 (11)	2·860 (9)	2·887 (19)
	3·005 (52)	3·251 (17)	3·290 (13)	3·299 (19)
	3·254 (32)	3·452 (11)	3·464 (9)	3·489 (13)
	3·449 (39)	3·297 (13)	3·304 (11)	3·285 (15)
–Cu(2)	2·435 (55)	2·160 (15)	2·140 (11)	2·067 (10)
	2× 2·625 (72)	2× 2·912 (19)	2× 2·945 (14)	2× 3·025 (12)
	2× 3·234 (43)	2× 3·474 (11)	2× 3·497 (8)	2× 3·570 (8)

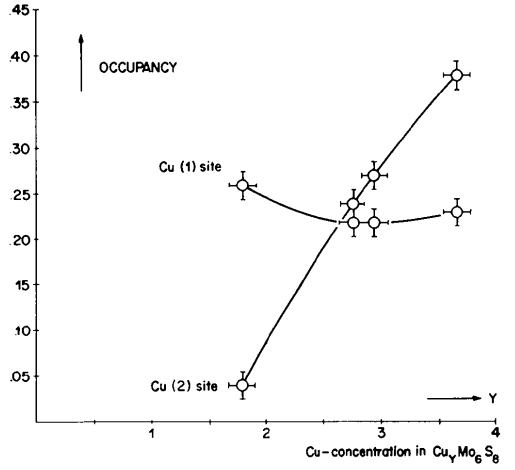

Fig. 3. Site occupancy of Cu(1) and Cu(2) as a function of the Cu concentration in $Cu_yMo_6S_8$ compounds ($y = 4 - 2x$).

tween Cu ions located on the peripheral sites of adjacent clusters and therefore acts in the direction of increasing occupancy for the inner sites. The relative importance of these two forces changes with the overall Cu concentration and this could explain the existence of the small minimum in the occupancy of site 1. This minimum cannot be located with precision from inspection of Fig. 1, but its existence seems to be confirmed by the variation of the distances with concentration between Cu atoms on site 1. Refinement of the occupancies of the S sites and inspection of a final difference map gave no indications of the existence of other defects.

Interatomic distances

All interatomic distances, except the Mo–Mo and Cu–Cu contacts, have values that are typical for Mo and Cu sulphides [Mo–S 2·35 (MoS_2), 2·36–2·57 (Mo_2S_3); Cu–S 2·1–2·3 (Cu_2S); S–S 3·64 (Cu_2S), 3·31–3·55 Å (Mo_3S_4)]. However, the Mo–Mo distances of 2·66–2·75 Å are among the shortest observed in compounds with fractional Mo–Mo bonds. They are smaller than in the pure metal (2·72 Å), in Mo_2S_3 (2·85 Å) and in high-melting carbides such as Mo_2C (3·00 Å). Shorter Mo–Mo distances are found in $MoCl_2$ (2·61 Å, Schäfer, von Schnering, Tillack, Kuhnen, Wöhrle & Baumann, 1967), a compound which also contains isolated Mo_6 octahedra, and in *A*15-type compounds in which the Mo atoms form infinite linear chains (d_{Mo-Mo} = 2·45–2·48 Å). By comparison, the extremely short Mo–Mo distance of 2·11 Å observed in $Mo_2Cl_8^{4-}$ complexes (Brencic & Cotton, 1969) is believed to correspond to a quadruple bond.

Variation of interatomic distances with Cu *concentration*

From Table 3, the following conclusions can be drawn. The distances generally increase with concentration, the Mo–S distances by 1·3% and the S–S distances by 1·1% on average. There are, however, two notable exceptions. Firstly, the Mo–Mo distances decrease on average by 1·7% from $Cu_{0.90}Mo_3S_4$ to $Cu_{1.83}Mo_3S_4$, or by 4·0%, if one compares analogous distances between $Cu_{1.83}Mo_3S_4$ and binary Mo_3S_4. This decrease corresponds to an anisotropic contraction of the Mo_6 octahedron such that the Cu-rich compound shows the smallest and most regular octahedron.

The second exception concerns the nearest-neighbour distances of Cu on site 1. Contrary to the evolution of the Cu–S distances around site 2, the distances first increase and then decrease slightly with Cu concentration. This behaviour is correlated with the anomalous variation of the occupancy of this site and

seems to confirm the existence of the minimum of occupancy discussed previously.

Vibrational parameters

The thermal parameters reveal interesting features. For Mo the longest principal axis of the ellipsoid of thermal vibration is tangential to a circle whose plane is perpendicular to **c**. Further, the low values of the U_{ij} cross-terms involving **1** make it obvious that the third principal axis lies close to the direction of $\mathbf{c}_{hex}$. The Mo_6 octahedron may therefore be regarded as a rigid unit that oscillates mainly around its ternary axis and vibrates along **c**. The amplitudes and directions of these vibrations are affected only to a small extent by the Cu concentration.

Analysis of the ellipsoids of thermal vibration for the Cu atoms reveals mobilities that are an order of magnitude higher than those of the Mo_6S_8 units. The principal axes of the ellipsoids are nearly parallel for both atoms and the direction of strongest vibration (r.m.s. amplitude = 0·3 Å) is found to occur from site 1 to site 2 and *vice versa* (Fig. 3). In view of their close proximity, they may not be occupied simultaneously. It is therefore probable that the Cu atoms are migrating between site 1 and site 2 even at room temperature. They move less easily between adjacent clusters and ionic d.c. conduction is therefore expected to set in at higher temperatures only.

Ionic–covalent bonding model

Two observations are significant for the establishment of an idealized bonding model. Firstly, the existence of an upper phase limit close to the composition $Cu_2Mo_3S_4$ and secondly, the contraction of the Mo_6 octahedron with increasing Cu content. The latter observation can be interpreted by assuming filling of partially occupied bond orbitals localized between the Mo atoms, the Cu atoms acting as electron donors. Since the distance between Cu and Mo is large enough to exclude direct bonding, the cluster Mo_6S_8 should be regarded as a pseudo-atom acting as an electron acceptor. Only four electrons are necessary to fill the Mo–Mo bond orbitals completely, leading to the ionic formula $Cu_4^+[Mo_6^{2+}S_8^{2-}]^{4-}$ at the upper limit of Cu concentration. This bonding model implies monovalent Cu and neglects any covalency effects other than Mo–Mo single bonds.

References

BADER, S. D., KNAPP, G. S., SINHA, S. K., SCHWEISS, P. & RENKER, B. (1976). *Phys. Rev. Lett.* **37**, 344–348.

BRENCIC, J. V. & COTTON, F. A. (1969). *Inorg. Chem.* **8**, 7–10.

CHEVREL, R. (1974). Thesis, series B, No. 186/112, Univ. of Rennes, France.

CHEVREL, R., SERGENT, M. & PRIGENT, J. (1971). *J. Solid State Chem.* **3**, 515–519.

FISCHER, Ø. (1974). *Colloq. Int. CNRS*, **242**, 79–85.

FISCHER, Ø., ODERMATT, R., BONGI, G., JONES, H., CHEVREL, R. & SERGENT, M. (1973). *Phys. Lett.* **45A**, 87–88.

FISCHER, Ø., TREYVAUD, A., CHEVREL, R. & SERGENT, M. (1975). *Solid State Commun.* **17**, 721–724.

FLÜKIGER, R., DEVANTAY, H., JORDA, J. L. & MULLER, J. (1977). *IEEE Trans. Magn.* **13**, 818–820.

GUILLEVIC, J., BARS, O. & GRANDJEAN, D. (1973). *J. Solid State Chem.* **7**, 158–162.

GUILLEVIC, J., BARS, O. & GRANDJEAN, D. (1976). *Acta Cryst.* B**32**, 1338–1342.

GUILLEVIC, J., LESTRAT, H. & GRANDJEAN, D. (1976). *Acta Cryst.* B**32**, 1342–1345.

International Tables for X-ray Crystallography (1974). Vol. IV, Birmingham: Kynoch Press.

JOHNSON, C. K. (1965). *ORTEP*. Report ORNL-3794 (version of the XRAY 76 system). Oak Ridge National Laboratory, Tennessee.

KIMBALL, C. W., WEBER, L., VAN LANDUYT, G., FRADIN, F. Y., DUNLAP, B. D. & SHENOY, G. K. (1976). *Phys. Rev. Lett.* **36**, 412–415.

LAWSON, A. C. (1972). *Mater. Res. Bull.* **7**, 773–776.

MAREZIO, M., DERNIER, P. D., REMEIKA, J. P., CORENZWIT, E. & MATTHIAS, B. T. (1973). *Mater. Res. Bull.* **8**, 657–668.

MATTHIAS, B. T., MAREZIO, M., CORENZWIT, E., COOPER, A. S. & BARZ, H. E. (1972). *Science*, **175**, 1465–1466.

SCHÄFER, H., VON SCHNERING, H.-G., TILLACK, J., KUHNEN, F., WÖHRLE, H. & BAUMANN, H. (1967). *Z. anorg. allgem. Chem.* **353**, 281–312.

SHELTON, R. N., LAWSON, A. C. & JOHNSTON, D. C. (1975). *Mater. Res. Bull.* **10**, 297–302.

VISWANATHAN, R. & LAWSON, A. C. (1972). *Science*, **177**, 267–268.

XRAY system (1976). Version of 1976, edited by J. M. STEWART. Tech. Rep. TR-446. Computer Science Center, Univ. of Maryland, College Park, Maryland.